Novel structural features and phase transition behaviour of $(Sr_{1-x}Ca_x)TiO_3$: I. Neutron diffraction study

Novel structural features and phase transition behaviour of $(Sr_{1-x}Ca_x)TiO_3$: I. Neutron diffraction study

Rajeev Ranjan†, Dhananjai Pandey†, V Siruguri‡, P S R Krishna§ and
S K Paranjpe§

† School of Materials Science and Technology, Institute of Technology, Banaras Hindu
University, Varanasi-221005, India
‡ Inter-University Consortium for DAE Facilities, Bhabha Atomic Research Centre, Trombay,
Mumbai 400085, India
§ Solid State Physics Division, Bhabha Atomic Research Centre, Trombay, Mumbai 400085,
India

Abstract. Superlattice reflections observed for the first time in the room temperature powder neutron diffraction patterns of SCT ($Sr_{1-x}Ca_xTiO_3$, $x \geqslant 0.12$) are shown to arise due to tilting of TiO_6 octahedra. Rietveld refinement of the neutron diffraction data confirms that the structure of SCT for $x \geqslant 0.12$ is orthorhombic similar to that of $CaTiO_3$. Implications of the presence of tilted TiO_6 octahedra and the associated off-centre displacements of Sr^{2+}/Ca^{2+} in SCT are discussed in detail with regard to the quantum ferroelectric behaviour of SCT at low temperatures. Structural phase transitions in SCT with $x = 0.06$ and 0.12 are also reported.

1. Introduction

Strontium titanate has been the paradigm of studies related to structural phase transitions and critical phenomena for the last few decades [1, 2]. It undergoes an antiferrodistortive phase transition due to the softening of a zone boundary phonon mode around 105 K [3]. On lowering the temperature below 105 K, its dielectric constant increases up to about 4 K because of the softening of the zone centre optical phonon. However, the dielectric constant below 4 K remains nearly constant and does not exhibit a ferroelectric phase transition on further lowering of the temperature as verified up to 35 mK [4]. Accordingly, $SrTiO_3$ (ST) has been termed as an incipient ferroelectric [4] with a Curie temperature close to 35 K. It has also been termed as a quantum paraelectric [4] since quantum fluctuations are believed to be responsible for precluding the condensation of the zone centre phonon and thereby suppressing the ferroelectric phase transition. Recently, there has been a revival of interest [5] in this material after the suggestion of Muller *et al* [6] about the possibility of a quantum phase transition below 36 K in close analogy to the coherent quantum state (CQS) in liquid He II [7].

Application of external stress [8] or electric field [9] is known to induce bulk ferroelectricity in ST at low temperatures. In addition, chemical substitution of Sr^{2+} by Ca^{2+} in very small concentrations has also been shown by Bednorz and Muller [10] to stabilize X–Y type ferroelectricity above a critical calcium concentration of $x_c = 0.0018$. The transition temperature (T_c) in $Sr_{1-x}Ca_xTiO_3$ (SCT) increases rapidly to 35 K with increasing calcium content up to $x_c = 0.016$ and then levels off following a relationship $T_c(x) = (x - x_c)^{0.5}$ for the quantum ferroelectric transitions. For $x \geqslant 0.016$, smearing of the ϵ'–T plot is observed.

This smearing increases while the peak value of ϵ' at the transition temperature decreases respectively with increasing Ca^{2+} content. This has been attributed [10] to the transition into a random field induced domain state with glassy aspects [11, 12]. Muller *et al* [6] have proposed that Ca^{2+} impurities may act as pinning centres for the dynamic quantum domains of the CQS. More recently, experimental evidence and arguments have been advanced [11, 13] in support of nanometric ferroelectric domains within microscopic ferroelastic domains which are supposed to have originated from an interaction of coherent acoustic quantum fluctuations with ferroelectric domains.
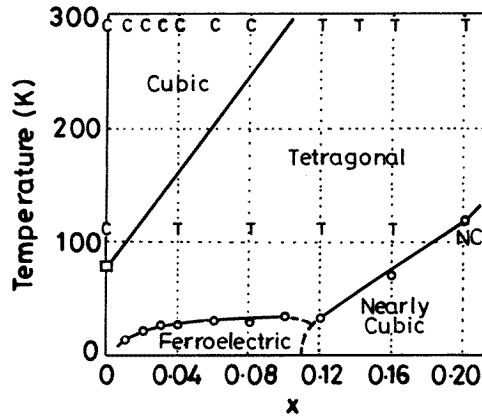

Figure 1. Phase diagram of $(Sr_{1-x}Ca_x)TiO_3$ given by Mitsui and Westphal.

The low temperature ferroelectric state in SCT has been assumed to be due to the off-centrality of Ca^{2+} similar to what is well known for the $K_{1-x}Li_xTaO_3$ (KLT) system with one important difference. In KLT, Li^+ is known [14, 15] to occupy off-centre positions along $\langle 001 \rangle_c$ of the cubic cell whereas Ca^{2+} is conjectured [12] to take up off-centre positions along $\langle 110 \rangle_c$. The off-centre occupancy of Li^+ in KLT has been confirmed in NMR studies [15]. No such experimental evidence exists for Ca^{2+} positions in SCT. Based on ionic size considerations, Bednorz and Muller [10] have proposed that some of the Ca^{2+} may also be located at the Ti^{4+} site. In order to maintain the overall charge neutrality, such a substitution will lead to $Ca^{2+}-V_O$ centres where V_O corresponds to a vacant oxygen site. $Ca^{2+}-V_O$ centres, if present, will form dipoles and can set up local random fields (RFs). The smearing of the $\epsilon'-T$ plots for $x \geqslant 0.016$ has been attributed [10] to the transition into a ferroelectric RF domain state. Such $Ca^{2+}-V_O$ centres have been reported in a related system, $Ba_{1-x}Ca_xTiO_3$ [16]. Even in ST, $Mn^{2+}-V_O$ centres have been observed by ESR [1]. There is however no experimental evidence for the presence of $Ca^{2+}-V_O$ centres in SCT.

Ca^{2+} substitution is known to raise the quantum ferroelectric transition temperature up to $x = 0.016$ only [10] while the 105 K antiferrodistortive transition temperature of pure ST is raised continuously up to much higher calcium concentrations ($x \approx 0.1$) for which measurements have been performed [17] (see figure 1). In a Raman scattering study on SCT single crystals with $x = 0.007$, Bianchi *et al* [18] have found that the antiferrodistortive transition occurs at 125 K. From a variation of refractive index with temperature for SCT single crystals with $x = 0.014$, Guzhva *et al* [19] have reported that the antiferrodistortive transition temperature to be 148 K. Taking 105 K as the transition temperature for pure ST, these studies suggest that the antiferrodistortive phase transition temperature should increase at a rate of $\sim$30 K per mol% addition of $CaTiO_3$ (CT). Unlike pure ST where the 105 K

transition is associated with the freezing of one of the triply degenerate R_{25} modes, CT shows [20] evidence for two transitions at 1423 K and 1523 K associated respectively with the freezing of the two of the triply degenerate R_{25} modes and M_3 mode. One would like to know the Ca^{2+} concentration at which there is a crossover from pure ST-like behaviour to CT-like in SCT. This is because the succession of CT-like antiferrodistortive transitions may also influence the quantum ferroelectric (QFE) behaviour of SCT at lower temperatures. The present investigation was undertaken to settle some of these issues structurally using powder neutron diffraction, x-ray diffraction, selected area electron diffraction and dielectric studies.

In part I of this series, we discuss neutron diffraction work in which we attempt to verify the off-centrality of Ca^{2+} ions and the presence of Ca^{2+}–V_O centres at the Ti^{4+}–O^{2-} positions using the crystal structure analysis approach. Although the quantum ferroelectric state in SCT is restricted to very low concentration of calcium ($0.0018 \leqslant x \leqslant 0.12$), any meaningful structure analysis work aimed at verifying the two different types of calcium occupancy in SCT has to be based on samples with sufficiently high calcium concentration. Since SCT is an isomorphous system with 100% solid solubility, one can unravel the site occupancy in ST matrix by using specimens with high calcium concentration. We present here the results of the first structure analysis work on the SCT system with $x = 0.50$, 0.25, 0.12 and 0.04 using Rietveld refinement of powder neutron diffraction data. It is shown for the first time that the structure of SCT is similar to that of CT for $x \geqslant 0.12$ in which Ca^{2+}/Sr^{2+} takes up off-centre positions because of the 'antiphase' tilting of TiO_6 octahedra. The 'antiphase' tilted TiO_6 octahedra give rise to superlattice peaks which are discernible on neutron diffraction patterns only and were completely missed in the earlier x-ray diffraction studies [17]. Neutron diffraction is ideally suited for verifying the presence of Ca^{2+} at the Ti^{4+} site also, since neutron scattering lengths of Ca and Ti ($b_{Ca} = 4.9$ fm, $b_{Ti} = -3.44$ fm) are of opposite signs, and the presence of the Ca^{2+} at the Ti^{4+} site would drastically change the scattering length of the Ti site. Our results indicate the absence of Ca^{2+} at the Ti^{4+} sites within the detection limit of our analysis. We also present the results of low temperature neutron diffraction studies on SCT samples for $x = 0.06$ and 0.12 to show that there is a crossover in the phase transition behaviour from pure ST to CT type somewhere in the composition range $0.06 < x \leqslant 0.12$.

2. Experiment

2.1. Structural characterization

The structural characterizations of the powder samples were carried out using XRD and neutron diffraction techniques. For XRD studies, a 12 kW Rigaku rotating anode powder diffractometer with Cu anode was used. Room temperature neutron diffraction data were collected using a neutron wavelength of 1.09 Å in the two theta range 10–80 degrees. A linear position sensitive detector based powder diffractometer ($\Delta d/d \sim 1\%$) at Dhruva Reactor, Trombay [21] was used in the above experiments. Low temperature neutron diffraction data were collected on the same spectrometer in the angular range of 10–60 degrees using an APD closed cycle refrigerator for $x = 0.06$ and 0.12.

2.2. Sample preparation

SCT powders were prepared by a semi-wet (SW) route [22] involving thermochemical reaction in a particulate mixture of TiO_2 and $Sr_{1-x}Ca_xCO_3$. $Sr_{1-x}Ca_xCO_3$ precursors for $x = 0.04$, 0.06, 0.12, 0.25 and 0.50 were prepared using ammonium carbonate solution as a precipitant in a stoichiometric mixture of strontium nitrate and calcium nitrate aqueous solutions. The

filtrates were checked for the absence of Sr^{2+} and Ca^{2+} using common analytical tests. The absence of cations in the filtrate confirmed the complete coprecipitation of Sr^{2+} and Ca^{2+} in the starting solution. X-ray diffraction studies confirmed the formation of $Sr_{1-x}Ca_xCO_3$ solid solutions. The use of chemically prepared $(Sr_{1-x}Ca_x)CO_3$ solid solution precursors ensures a uniform supply of Sr^{2+} and Ca^{2+} ions at the unit cell level at the time of reaction with TiO_2 particles.

For the synthesis of SCT powders, $(Sr_{1-x}Ca_x)CO_3$ precursors were first mixed with TiO_2 in stoichiometric proportion in a centrifugal ball mill with a zirconia jar and balls for 6 h. Acetone was used as a mixing medium. For the synthesis of ST and CT, $SrCO_3$ and $CaCO_3$ were milled with TiO_2 powders for the same duration. These ball milled powders were then calcined at 1373 K for 6 h. The calcined powders were again ball milled and then pelletized using cylindrical die of 1 cm diameter at a load of 60 kN with 2% PVA solution as a binder. Green pellets were sintered at 1573 K for 6 h. The powders obtained by crushing these sintered pellets were annealed at 873 K for removing strains induced by crushing before using them for diffraction studies. Room temperature XRD studies confirmed these powders to be monophasic.

3. Results and analysis

3.1. Neutron powder diffraction data

Figure 2 depicts the neutron powder diffraction patterns for $(Sr_{1-x}Ca_x)TiO_3$ powders with $x = 0.50, 0.25, 0.12$ and 0.04 over 2θ range 21.6 to 27.3 degrees. The diffractograms shown in figure 2 contain well resolved extra reflections (marked with X in the figure) which cannot be indexed with respect to the elementary cubic-perovskite cell for $x \geqslant 0.12$. The intensity of these extra reflections decreases with decreasing Ca^{2+} content up to $x = 0.12$. We first proceed to understand the origin of the extra reflections.

3.2. Possible origin of superlattice reflections

3.2.1. Role of Sr^{2+}/Ca^{2+} ordering in SCT50.
Superlattice reflections have been proposed to arise in mixed perovskites as a result of cationic ordering at the A and B sites of the ABO_3 structure [22, 23]. Differences in the valence of the atoms occupying the same site in the unit cell can promote chemical ordering in order to minimize [22] the electrostatic energy. Large differences (greater than 7% and less than 17%) [22] in the size of the cations occupying the same site in the unit cell can also promote chemical ordering in order to minimize the elastic strain energy. In the case of isovalent substitution, such as Ca^{2+} at the Sr^{2+} site in SCT, minimization of the elastic strain energy due to the difference in the ionic radii ($r_{Sr^{2+}} = 1.12$ Å, $r_{Ca^{2+}} = 0.99$ Å) can promote ordering of Sr^{2+} and Ca^{2+}. There can be three different possibilities for the 1:1 ordering of Sr^{2+}/Ca^{2+} in SCT50 similar to that suggested for $(Pb_{0.5}Ca_{0.5})TiO_3$ by King *et al* [23] resulting from the occupancy of alternate $\{111\}$, $\{110\}$ or $\{100\}$ type planes of the cubic structure by Sr^{2+} and Ca^{2+}. The space groups and orientation relationship of the ordered and the elementary perovskite unit cells for the three ordering schemes are as follows: (i) $\{111\}$ ordering: $Fm\bar{3}m$, $a_{ordered} = b_{ordered} = c_{ordered} = 2a_{perovskite}$; (ii) $\{110\}$ ordering: $P4mm$, $a_{ordered} = b_{ordered} = \sqrt{2}a_{perovskite}$, $c_{ordered} = c_{perovskite}$ and (iii) $\{100\}$ ordering: $P4mm$, $a_{ordered} = b_{ordered} = a_{perovskite}$; $c_{ordered} = 2c_{perovskite}$.

In order to see whether the superlattice reflections in figure 2 are due to 1:1 chemical ordering of Sr^{2+}/Ca^{2+}, we have simulated the neutron powder diffraction patterns for ordered
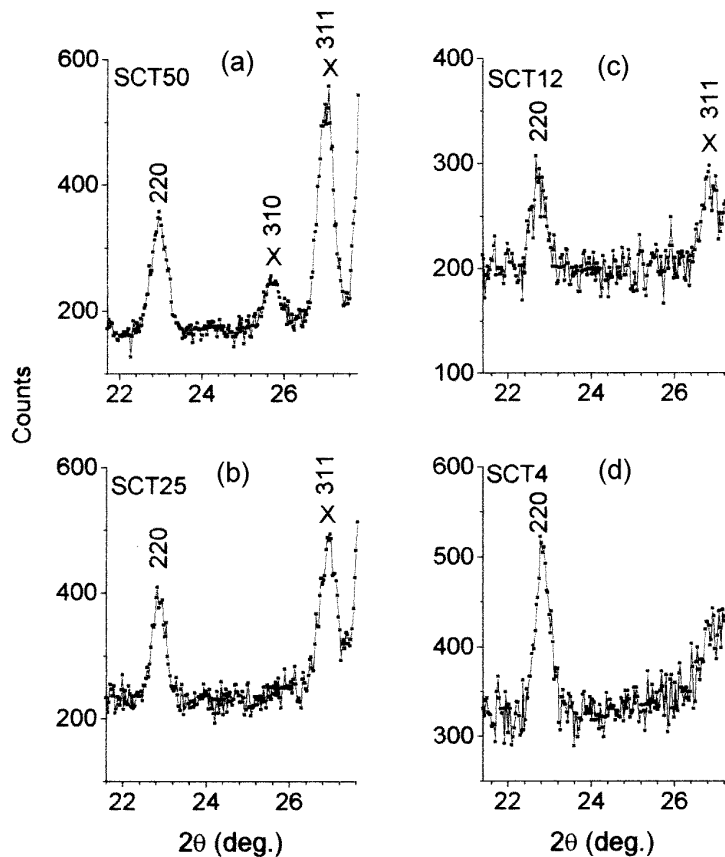
Figure 2. Part of the observed room temperature neutron diffraction pattern of $(Sr_{1-x}Ca_x)TiO_3$ for $x =$ (a) 0.50, (b) 0.25, (c) 0.12 and (d) 0.04 showing superlattice reflections for $x \geqslant 0.12$. The indices are with respect to a doubled pseudocubic cell.

SCT50 for the three ordering schemes mentioned above using the programme DBWS 9411 [24]. The simulated diffraction patterns are shown in figure 3. A comparison of the three simulated powder diffraction patterns with the experimentally observed pattern for SCT50, shown in the same figure, suggests that none of these ordering schemes can independently account for all the superlattice peaks observed experimentally. For example the $Fm\bar{3}m$ space group for {111} ordering requires extinction of reflections like 310, 312 (indexed on a doubled cubic cell), which are nevertheless present in the observed pattern. On the other hand, the $P4mm$ space group for {110} and {100} ordering cannot account for the prominent peaks in figure 3(d), such as 311, 331 etc. These observations thus rule out the possibility of the ordered arrangement of the Sr^{2+} and Ca^{2+} being responsible for the observed superlattice reflections for SCT50. As shown elsewhere [25], the superlattice reflections observed in $(Pb_{0.5}Ca_{0.5})TiO_3$ are also not due to chemical ordering of Pb^{2+} and Ca^{2+}.

3.2.2. Role of TiO$_6$ octahedral tilt. Superlattice reflections in perovskites can also result [26] from antiphase tilting of neighbouring TiO_6 octahedra. Glazer [26] has shown that these tilts can be described in terms of three component tilts (rotations) about the three tetrad axes

(namely a, b and c of the elementary cubic perovskite cell) of the TiO_6 octahedron. Each tilt about a given axis forces tilts of opposite sense about the other two tetrad axes leading to a doubling of the unit cell parameters in the two perpendicular directions. In addition, the octahedra along the tilt axis in the neighbouring unit cells may be tilted 'in phase' (+ve tilt) or 'antiphase' (−ve tilt). For antiphase tilting, the unit cell will be doubled along the axis of the tilt also. The 'in-phase' tilt gives rise [26] to superlattice reflections with one even and two odd indices with respect to the doubled pseudocubic cell. The antiphase tilt, on the other hand, leads to superlattice reflections with all odd indices. The various superlattice reflections observed in SCT50 (see figure 3(d)) have indices which are either all odd or one even and two odd. The observation of superlattice reflections with both types of index suggests the presence of 'in-phase' (+) as well as 'antiphase' tilts (−) in the SCT50 structure. A similar set of reflections has been reported [26] for pure CT also which belongs to the $a^- a^- c^+$ tilt system in the Glazer's classification scheme. It therefore appears likely that SCT is inheriting the tilt system of pure CT.

4. Rietveld refinement

Rietveld refinement of the powder neutron diffraction data was carried out for SCT ($x = 0.04$, 0.12, 0.25 and 0.50) as well as CT. The programme DBWS 9411 [24] was used for the profile refinements. In all the refinements, scale factor, zero correction, background parameters and half widths in addition to the lattice parameters (A_0, B_0, C_0), positional coordinates (X, Y, Z), occupancy (N) and isotropic thermal parameters (B) were varied. Refining the occupancy parameters of all the atoms together led to very high standard deviations. In order to overcome this problem, the occupancy parameters for the oxygen atoms had to be refined separately from the occupancy parameters for Sr, Ca and Ti atoms. The observed, calculated and difference profiles for CT, SCT50, SCT25, SCT12 and SCT4 are shown in figure 4.

The presence of odd–odd–odd (ooo) and odd–odd–even (ooe) types of reflections in the experimentally observed neutron diffraction pattern of CT confirms the presence of − and + tilts respectively in agreement with the earlier findings of Glazer [26]. The tilt system proposed by Glazer for this structure is $a^- a^- c^+$ and corresponds to the space group $Pbnm$ proposed by Kay and Bailey [27] in their XRD studies. We therefore refined the structure of CT using the $Pbnm$ space group.

Some of the superlattice reflections such as 320, 410 and 330 (marked with arrows in figure 4(a)), which were present in the neutron diffraction pattern for CT, are absent in the pattern for SCT50. However, as explained in the previous section, the remaining superlattice peaks still indicate the presence of − and + tilts similar to that for CT. Accordingly, the refinement for SCT50 was also carried out assuming the $Pbnm$ space group.

A comparison of the experimentally observed powder neutron diffraction patterns for SCT25 and SCT12 with that of SCT50 shows that some of the superlattice reflections like 310 and 312 (marked with arrows in figure 4(b)) are absent in the diffractograms for SCT25 and SCT12. This may be due to two different reasons. For the $a^- a^- c^+$ tilt system, it is possible that with decreasing calcium content, the tilt angles have become so small that the intensities of these superlattice peaks have become nearly zero. The absence of 'odd–odd–even' type reflection, on the other hand, may also be attributed to the absence of + tilt. In this situation, the tilt system for SCT25 and SCT12 can as well be $a^- a^- c^0$ belonging to the space group $Ibmm$. In order to make a choice between these two possibilities, we refined the structure of SCT25 using both the models. Refinement corresponding to the $a^- a^- c^0$ tilt system invariably led to slightly higher R_{wp} as compared to that for the $a^- a^- c^+$ tilt system. It was therefore concluded that the correct tilt system for SCT25 is $a^- a^- c^+$. The structure of SCT12 was also
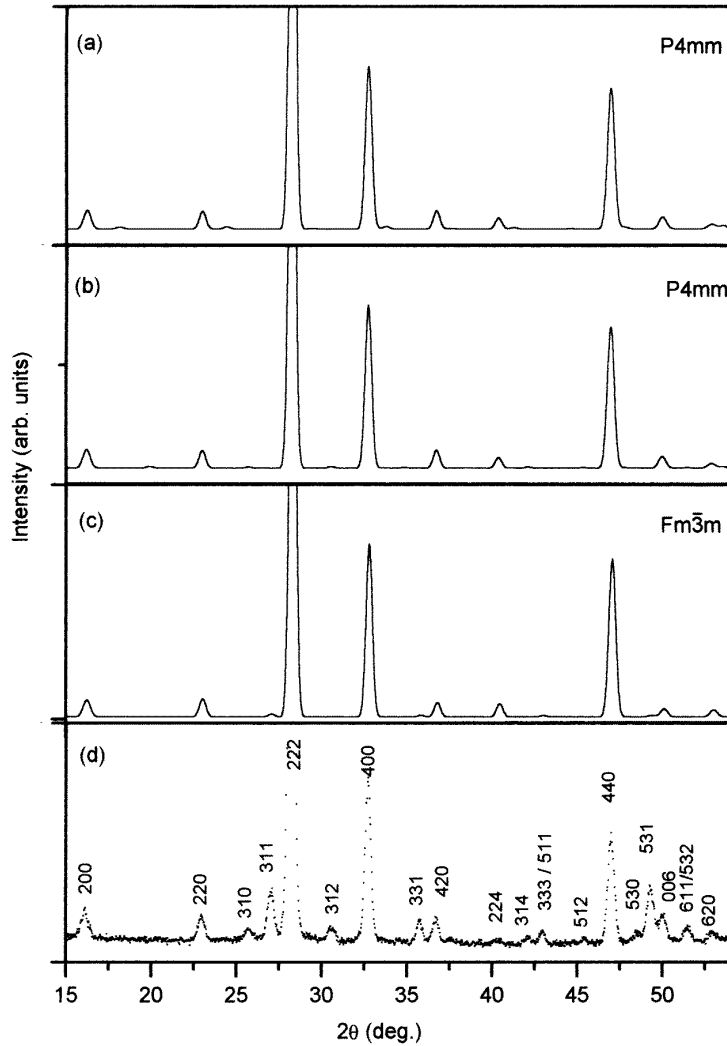
Figure 3. Simulated neutron diffraction pattern of SCT50 for (a) 100, (b) 110 and (c) 111 ordering schemes, and (d) observed neutron diffraction pattern of SCT50. The indices in (d) are with respect to a doubled pseudocubic cell ($2a \times 2b \times 2c$). The peak corresponding to the 222 reflection is truncated.

refined using $a^- a^- c^+$ as well as $a^- a^- c^0$ tilt systems. Both the models gave similar values as far as the refined structural parameters are concerned with the tilt angle γ being of the order of the standard deviation for the $a^- a^- c^+$ model. Thus the tilt system for SCT12 may be either $a^- a^- c^+$ or $a^- a^- c^0$. However, the refined positional coordinates are nearly the same for both the tilt systems.

It is evident from figure 2 that with increasing Sr^{2+} content the intensity of the 311 superlattice reflection decreases. For SCT4 also, there appears to be a rising trend in the intensity profile near the expected 311 position. However, it was not possible to attribute this rising trend to the presence of 311 reflection unambiguously on the basis of the present data. In the absence of any clear evidence for the superlattice reflections, we decided to analyse
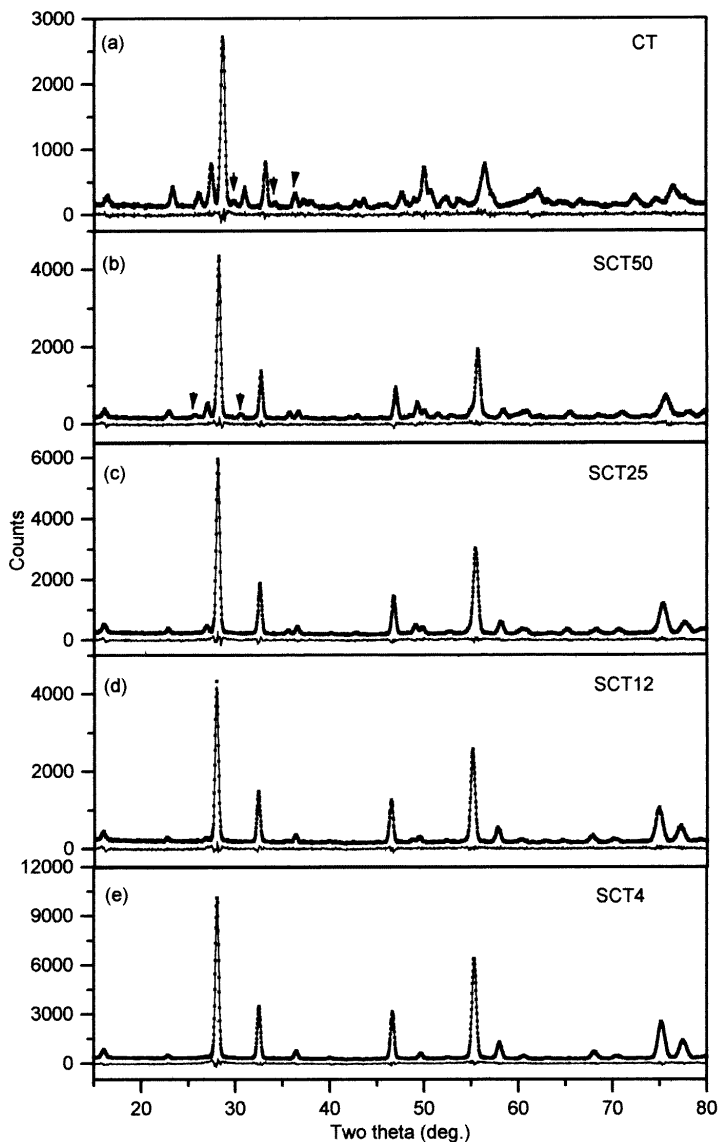
Figure 4. Observed ($\cdots$), calculated (——) and difference neutron powder diffraction patterns of $CaTiO_3$ and SCT.

the observed data in terms of the cubic perovskite structure with space group $Pm3m$. Our findings will however remain tentative until the availability of higher resolution powder neutron diffraction data.

In all cases, satisfactory R-factors were obtained after refinement. The refined structural parameters and R-factors for CT, SCT50, SCT25 and SCT12 are given in table 1. The refined structural parameters and R-factors for SCT4 are as follows:

$a = 3.9092(1)$ Å $B_{Sr/Ca} = 0.41(3)$ Å^2 $B_{Ti} = 0.19(4)$ Å^2 $B_O = 0.56(2)$ Å^2

$R_p = 4.91$ $R_{wp} = 7.22$ $R_B = 3.17$ $R_E = 4.29$.

The tilt angles for the TiO$_6$ octahedra as obtained from the refined oxygen coordinates are also given in table 1. Figure 5 shows the variation of the tilt angles (α and γ) as a function of calcium concentration. Evidently, the tilt angles α and γ decrease with decreasing calcium content.
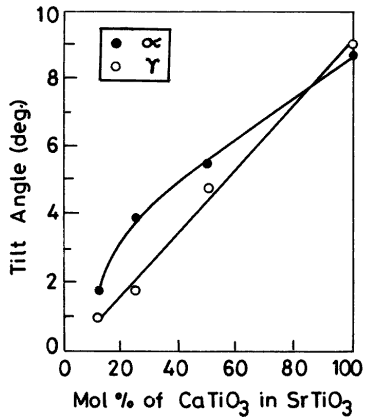

Figure 5. Variation of tilt angles α and γ of the TiO$_6$ octahedra in SCT with calcium content. The continuous line is drawn to show the trend.

Table 1. Refined structural parameters (space group: *Pbnm*) of (Sr$_{1-x}$Ca$_x$)TiO$_3$ for $x = 1.00$, 0.50, 0.25 and 0.12 at room temperature. R_p, R_{wp}, R_B and R_E are profile, weighted profile, Bragg and expected R-factors, respectively.

	Occupancy	Positional coordinates			Thermal parameters
	N	X	Y	Z	B (Å^2)
Sr/Ca	$N_{Ca} = 0.999(6)$	$-0.006(1)$	$0.5344(7)$	0.250	$0.70(5)$
	$N_{Sr} = 0.499(5)$ $N_{Ca} = 0.494(7)$	$-0.005(3)$	$0.514(1)$	0.250	$0.52(5)$
	$N_{Sr} = 0.750(5)$ $N_{Ca} = 0.245(8)$	$-0.001(3)$	$0.514(1)$	0.250	$0.41(4)$
	$N_{Sr} = 0.880(6)$ $N_{Ca} = 0.122(9)$	$-0.002(4)$	$0.510(1)$	0.250	$0.43(4)$
Ti	$N_{Ti} = 1.000$	0.000	0.000	0.000	$0.21(6)$
	$N_{Ti} = 1.000$	0.000	0.000	0.000	$0.36(6)$
	$N_{Ti} = 1.000$	0.000	0.000	0.000	$0.24(6)$
	$N_{Ti} = 1.000$	0.000	0.000	0.000	$0.19(6)$
O1	$N_{O1} = 1.003(9)$	$-0.0698(9)$	$-0.0155(6)$	0.250	$0.63(6)$
	$N_{O1} = 0.99(2)$	$-0.054(1)$	$-0.008(2)$	0.250	$1.6(2)$
	$N_{O1} = 1.00(1)$	$-0.041(1)$	$-0.004(2)$	0.250	$1.4(1)$
	$N_{O1} = 1.01(2)$	$-0.024(2)$	$-0.005(2)$	0.250	$1.3(1)$
O2	$N_{O2} = 2.01(1)$	$0.2104(4)$	$0.2893(4)$	$0.0384(4)$	$0.52(3)$
	$N_{O2} = 2.00(2)$	$0.228(1)$	$0.270(1)$	$0.0241(5)$	$0.25(6)$
	$N_{O2} = 2.00(2)$	$0.240(2)$	$0.255(3)$	$0.0170(5)$	$0.36(5)$
	$N_{O2} = 1.99(2)$	$0.244(4)$	$0.254(6)$	$0.0080(4)$	$0.18(5)$

x	Cell parameters (Å)			Tilt angle (deg.)		R-factors			
	A_0	B_0	C_0	$\alpha = \beta$	γ	R_p	R_{wp}	R_B	R_E
1.00	5.3827(5)	5.4537(5)	7.6551(9)	8.7(1)	9.0(1)	5.92	7.94	4.71	6.77
0.50	5.498(1)	5.491(1)	7.753(1)	5.5(1)	4.8(2)	6.00	8.08	6.49	6.11
0.25	5.525(2)	5.522(2)	7.7763(9)	3.9(1)	1.8(6)	5.55	7.56	6.44	5.31
0.12	5.552(2)	5.546(3)	7.836(2)	1.8(1)	1(1)	5.30	7.31	5.33	6.03

The 12-fold cuboctahedral coordination of the A site cation in the ABO_3 structure is severely distorted for pure CT since eight of the twelve O^{2-} ions are located at an average bond length of 2.499 Å while the remaining four are at a distance of 3.116 Å. With increasing Sr^{2+} concentration, the difference between the average nearest neighbour and next nearest neighbour bond lengths decreases. The average A^{2+}–O^{2-} bond lengths for the nearest and the next nearest neighbours for SCT50, SCT25 and SCT12 are 2.902, 2.848 and 2.826, and 2.537, 2.620 and 2.686 Å respectively. For SCT4, the Sr^{2+}/Ca^{2+}–O^{2-} bond length is equal to 2.764 Å. In contrast to the Sr^{2+}/Ca^{2+}–O^{2-} bond lengths, the Ti^{4+}–O^{2-} bond lengths are nearly the same ($\sim$1.95 Å) for pure CT as well as for SCT compositions. This indicates that the TiO_6 octahedral cage remains undistorted, justifying the description of the overall structure in terms of rigid octahedral tilts.

5. Phase transitions in SCT

We have also investigated the structural phase transitions in SCT6 and SCT12 by monitoring the evolution of the 531 superlattice reflection at low temperatures. This reflection is absent in the room temperature pattern of SCT6 but appears just below room temperature. For SCT12, the 531 superlattice reflection is already present even at room temperature. However, its intensity gradually increases below room temperature. Figure 6 depicts the evolution of the peak intensity of the 531 superlattice reflection normalized with respect to its neighbouring 006 perovskite reflection as a function of temperature for SCT6 and SCT12. For both cases, the intensity of the 531 superlattice reflection increases up to about 150 K below which it tends to stabilize. From an extrapolation of the curve for SCT12 in figure 6 to zero intensity value, the antiferrodistortive phase transition temperature is expected to be around 375 K whereas it is around 300 K for SCT6.
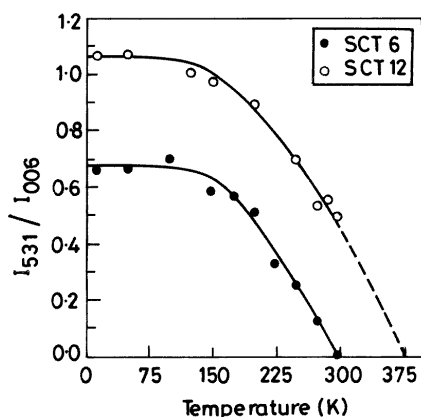

Figure 6. Variation of I_{531}/I_{600} with temperature for SCT6 and SCT12. The continuous line is drawn to show the trend.

Figure 7 shows diffraction profiles of 531 and 006 reflections for SCT6 and SCT12 at three representative temperatures. The diffraction patterns remain unchanged on going from 100 to 12 K for both SCT6 and SCT12 (figure 7). We do not observe any signature of peak splitting for the main perovskite reflection in the quantum ferroelectric regime to the resolution of our spectrometer. The resolution of the present data is not sufficient to study the variation in the structural parameters as a function of temperature. In fact, the only significant change in going below room temperature is the appearance of new superlattice reflections for SCT6 or enhancement in the intensity of the existing superlattice reflections for SCT12 up to about 150 K. However, the intensity changes are so small

that no meaningful change in the structural parameters could be detected by Rietveld analysis of the data at various temperatures. We have however found that the thermal parameters of the Sr/Ca decrease with temperature and their positions are nearly frozen below 100 K.

6. Discussion

6.1. Room temperature crystal structure

Mitsui and Westphal [17] in their XRD studies determined the unit cell parameters of SCT ($0 \leqslant x \leqslant 0.20$) from the observed splitting of the 422 cubic perovskite reflection and concluded that the structure of SCT is tetragonal for $x > 0.10$. As per their phase diagram (see figure 1) the room temperature tetragonal structure for $x > 0.10$ is similar to the tetragonal structure of ST below 105 K. Our neutron diffraction patterns for SCT with $x \geqslant 0.12$ show a large number of superlattice reflections which were not observed in the XRD patterns by Mitsui and Westpahl because of the low scattering length of oxygen for the x-rays. Refinement of the structure taking into account all the superlattice reflections along with the perovskite reflections clearly reveals an orthorhombic symmetry even though the refined unit cell parameters do indicate a pseudotetragonal lattice. Thus the present work has clearly established that the room temperature structure of SCT is orthorhombic (CT-like) for $x \geqslant 0.12$ whereas it is cubic (ST-like) for $x \leqslant 0.06$.

6.2. Antiferrodistortive phase transitions

From the evolution of the 531 superlattice reflection and 006 perovskite reflection as a function of temperature, we find that the antiferrodistortive transition temperature for SCT6 should be somewhere between 300 and 275 K. As mentioned earlier, the antiferrodistortive phase transition temperatures for SCT0.7 and SCT1.4, as obtained by Bianchi *et al* [18] and Guzhva *et al* [19], suggest that the transition temperature increases at a rate of ∼30 K per mol% addition of CT in ST. At this rate, one expects a transition temperature of 290 K for SCT6 which is in reasonable agreement with our findings. This in essence suggests that the phase transition behaviour of SCT remains ST-like up to 6 mol% of Ca. In contrast, the transition temperature of 373 K for SCT12 is lower than the transition temperature expected on the basis of $dT_c/dx \sim 30$ K/mol% of CT in ST. A high temperature XRD study of the phase transition behaviour of SCT12, described in part II of this series, shows that the structure indeed becomes cubic around 375 K in close agreement with the T_c determined from the disappearance of the 531 superlattice reflection in neutron diffraction patterns. Thus, there is a departure from the linear variation of T_c with x which seems to have occurred for a composition somewhere between $x = 0.06$ and 0.12. This may be due to a crossover from the ST-like phase transition behaviour for SCT6 to CT-like behaviour for SCT12 as confirmed by high temperature XRD studies in part II for $x \geqslant 0.12$.

6.3. Structure of the QFE phase

Mitsui and Westphal [17] have proposed that the structure of SCT for $x > 0.10$ in the quantum ferroelectric regime is pseudocubic (see figure 1). The neutron diffraction patterns given in figures 7 show that the intensity of the superlattice reflection gradually increases below the antiferrodistortive phase transition temperature. This is because of the evolution of the order parameter as well as the relief in the extinctions due to domain formation [2]. This increasing tendency nearly levels off at temperatures (∼150 K) well above the quantum ferroelectric phase
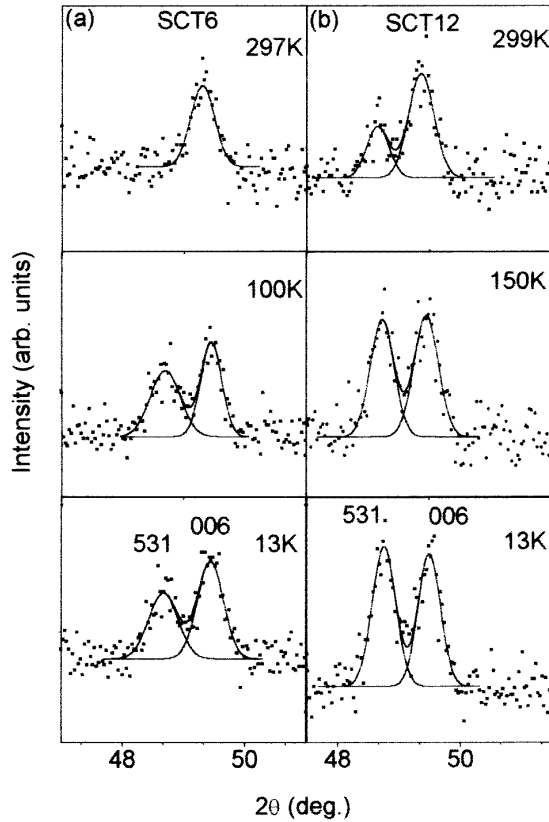
Figure 7. Profiles of 531 and 006 (doubled pseudocubic indices) pair of reflections of SCT6 and SCT12 at three representative temperatures.

transition temperature reported by Bednorz and Muller for SCT6 and SCT12. The fact that the superlattice reflections originating from the antiferrodistortive phase transitions persist even in the QFE regime (see the diffractogram at 13 K in figure 7) clearly rules out the suggestion of Mitsui and Westphal that the structure of the QFE phase should be cubic/pseudocubic. It is, however, certain that the space group for the QFE phase cannot be *Pbnm* which is centrosymmetric. Since we do not find any perceptible change in the entire diffraction pattern in going from 100 K to 13 K, it suggests that the change in the atomic positions occurring with the freezing of the $q = 0$ mode is either too small to be resolved with our spectrometer or is occurring over mesoscopic length scales. Dielectric spectroscopic studies on SCT samples with $x \geqslant 0.002$ [11] also suggest the absence of global phase transition in the QFE regime and point towards glassy character of the QFE phase for which one normally does not expect any signature of global symmetry breaking [14]. From a Rietveld analysis of x-ray and neutron powder diffraction data for pure ST at 1.5 K, Kiat and Roisnel [30] have also suggested the absence of global symmetry breaking in ST.

6.4. Origin of quantum ferroelectric behaviour

As pointed out in section 1, the stabilization of the ferroelectric phase in SCT against the quantum fluctuations has all along been attributed to the off-centre location of the Ca^{2+} ions in

the cubooctahedral cage of O^{2-} ions. Our results have shown that the off-centre displacement of the Ca^{2+}/Sr^{2+} in the $\langle 110 \rangle$ cubic direction in SCT occurs because of the antiphase tilting of the TiO_6 octahedra in the neighbouring unit cell. This is similar to what is well known [26] for CT with one important difference. In pure CT, neighbouring octahedra are tilted in opposite sense in order to minimize the strain field associated with the individual corner-sharing TiO_6 octahedra. In SCT, the tilted octahedra associated with calcium containing unit cells seem to force the tilting of the octahedra associated with strontium containing unit cells also in order to minimize the strain energy as confirmed by the presence of the characteristic superlattice reflections in the neutron diffraction patterns for $x \geqslant 0.12$. If the adjacent octahedra tilt in opposite sense by nearly the same amount, the A-site cations (Sr^{2+} and Ca^{2+}) will undergo equal and opposite off-centre displacements along the cubic [110] and [1$\bar{1}$0] directions on alternate cubic (001) planes. In such a situation, the antiparallel local dipole moments generated by the adjacent off-centre cations will cancel each other. In SCT samples with larger strontium concentration, the tilting of the TiO_6 is initiated at the Ca^{2+} site and propagated away from it through the corner-shared TiO_6 octahedra. However, the tendency of the Sr^{2+} ions to maintain a 12-fold oxygen coordination with an untilted TiO_6 octahedral configuration will cause the magnitude of the tilt of the octahedra to decrease gradually as one moves away from the Ca^{2+} site. This gradual decrease of the tilt of the TiO_6 octahedra associated with Sr^{2+} containing unit cells will in turn decrease the magnitude of the off-centre displacements of the Sr^{2+} ions the farther it is located from the site of the maximum tilt, i.e., the site of the Ca^{2+}. The dipole moments associated with the antiparallel but unequal off-centre displacements of the A-site cations at different points in space will therefore not cancel each other leaving behind a net local dipole moment. Thus, even though the strain fields due to the TiO_6 octahedra associated with Ca^{2+} containing unit cells may interact weakly through the corner-shared octahedra to give rise to long range cooperative tilt through out the matrix, it may leave behind net dipole moment in neighbouring regions due to unequal off-centre displacements of A-site cations. If the tilted TiO_6 octahedra associated with Ca^{2+} containing unit cells are far too apart to let their strain fields overlap, the cooperative anti-phase tilting of the octahedra throughout the matrix may not occur. This may account for the absence of superlattice reflections for lower Ca^{2+} concentration such as for SCT4 and SCT6. This does not necessarily imply that the structure of SCT4 is cubic locally. In fact, even in SCT4 and SCT6, there will be small regions centred around Ca^{2+} ions in which the Sr^{2+} ions would have locally undergone antiparallel off-centre displacements with gradually decreasing magnitudes. In such cases also, the pairwise cancellation of the local dipole moments due to the off-centred cations will never be total and it will invariably leave behind a net local dipole moment in random directions. Since these random site dipoles are embedded in a dielectrically soft ST matrix, they will carry a polarization cloud whose size will grow with decreasing temperature until these polar regions start overlapping and bring about a percolative type phase transition [13]. These polar regions are also responsible for the dielectric relaxations observed by several workers [11, 12] in the SCT system.

Acknowledgments

References

[1] Scott J F 1974 *Rev. Mod. Phys.* **46** 83
[2] Cowley R A 1980 *Adv. Phys.* **29** 1
[3] Unoki H and Sakudo T 1967 *J. Phys. Soc. Japan* **23** 546
　　Shapiro S M, Axe J D and Shirane G 1972 *Phys. Rev.* B **6** 4332
　　Liu M, Finlayson T R and Smith T F 1997 *Phys. Rev.* B **55** 3480
　　Muller K A, Berlinger W and Waldner F 1968 *Phys. Rev. Lett.* **21** 814
[4] Muller K A and Burkard H 1979 *Phys. Rev.* B **19** 3593
[5] Vacher R, Pelous J, Hennion B, Goddens G, Courtens E and Muller K A 1992 *Europhys. Lett.* **17** 45
　　Nes O M, Muller K A, Suzuki T and Fossheim F 1992 *Europhys. Lett.* **19** 397
　　Viana R, Lukenheimer P, Hemberger J, Bohmer R and Loidl A 1994 *Phys. Rev.* B **50** 601
[6] Muller K A, Berlinger W and Tosatti E 1991 *Z. Phys.* B **84** 277
[7] Henshaw D G and Woods A D B 1961 *Phys. Rev.* **121** 1266
[8] Uwe H and Sakudo T 1976 *Phys. Rev.* B **13** 271
　　Fuji Y, Uwe H and Sakudo T 1987 *J. Phys. Soc. Japan* **56** 1940
[9] Hemberger J, Luckenheimer P, Viana R, Bohmer R and Loidl A 1995 *Phys. Rev.* B **52** 13 159
[10] Bednorz J G and Muller K A 1984 *Phys. Rev. Lett.* **52** 2289
[11] Dec J, Kleeman W, Bianchi U and Bednorz J G 1995 *Europhys. Lett.* **29** 31
　　Bianchi U, Dec J, Kleeman W and Bednorz J G 1995 *Phys. Rev.* B **51** 8737
[12] Kleeman W and Schremmer H 1989 *Phys. Rev.* B **40** 7428
[13] Kleeman W, Bianchi U, Burgel A, Prasse M and Dec J 1995 *Phase Transitions* **55** 57
[14] Vugmeister B E and Glinchuk M D 1990 *Rev. Mod. Phys.* **62** 993
　　Hochli U T, Knorr K and Loidl A 1990 *Adv. Phys.* **39** 599
[15] Borsa F, Hochli U T, Vander Klink J J and Rytz D 1980 *Phys. Rev. Lett.* **45** 1884
[16] Krishna P S R, Pandey D, Tiwari V S, Chakravarty R and Dasannacharya B A 1993 *Appl. Phys. Lett.* **62** 231
　　Tiwari V S and Pandey D 1994 *J. Am. Ceram. Soc.* **77** 1819
[17] Mitsui T and Westphal W B 1961 *Phys. Rev.* **124** 1354
[18] Bianchi U, Kleeman W and Bednorz J G J 1997 *J. Phys.: Condens. Matter* **6** 1239
[19] Guzhva M E, Markovin P A and Kleeman W 1997 *Phys. Solid. State* **39** 625
[20] Redfern S A T 1996 *J. Phys.: Condens. Matter* **8** 8267
[21] Paranjpe S K 1989 *Ind. J. Pure Appl. Phys.* **27** 578
[22] Setter N and Cross L E 1980 *J. Mater. Sci.* **15** 2478
[23] King G, Goo E, Yamamoto T and Okazaki K 1988 *J. Am. Ceram. Soc.* **71** 454
[24] Young R A, Sakthivel A, Moss T S and Paiva Santos C O 1994 *Program DBWS-9411 for Rietveld Analysis of X-ray and Neutron Powder Diffraction Pattern*
[25] Rajeev Ranjan, Neelam Singh, Pandey D, Siruguri V, Krishna P S R, Paranjpe S K and Banerjee A 1997 *Appl. Phys. Lett.* **70** 3221
[26] Glazer A M 1972 *Acta. Crystallogr.* B **28** 3384
　　Glazer A M 1975 *Acta. Crystallogr.* A **31** 756
[27] Kay H F and Bailey P C 1957 *Acta. Crystallogr.* **10** 1957
[28] Kiat J M and Roisnel T 1996 *J. Phys.: Condens. Matter* **8** 3471